HiSST: International Conference on
High-Speed Vehicle Science Technology
26–29 November 2018, Moscow, Russia

Characterisation of combustion oscillations in a cavity flame holder during acceleration experiments

H. Lian[1], HB. Gu[1], LJ. Yue[1], YX. Zhou[1], XY. Chang[1]

Abstract

The combustion oscillation characteristics are investigated in a dual-mode model combustor equipped with cavity flameholders during acceleration experiments. The combustion oscillations are measured by a spark plug sensor at 200kHz. The spark plug sensor with fast response is preferable due to the short timescale associated in supersonic combustors. Its high sensitivity to flame dynamics also provides additional information other than the wall pressure measurement at conditions when minor pressure change occurs. Nonlinear analysis is performed to evaluate the deterministic and random nature of transient flame dynamics. Strong deterministic behavior is observed for the first time that positively supports further evaluation and development of predictive flame dynamics model.

Keywords: *transient operation, supersonic combustor, combustion oscillation, nonlinear analysis*

1. Introduction

It is widely known that the shock interaction with shear layers significantly affects the pressure oscillations and induces combustion instabilities [Sun et al. 2008], yet combustion oscillations in a supersonic combustor are also found to be greatly affected by transverse jet injection, main flow shock trains and coherent turbulent flow structures [Curran et al. 1996]. It is not clear which of the mechanisms dominates the flow flame interaction that could result in flashback and eventually engine unstart, especially during transient accelerating operations. Thus, experiments are designed to evaluate the shock train interaction with combustion oscillations in a cavity flame holder based on a unique facility of the CAS transient operation wind tunnel, which forms the goal of the paper.

The first step towards dismantling the multi-physics phenomena requires statistical characterization of the combustion oscillation. The flame spread angle and the reaction zone leading edge derived from chemiluminescent images acquired through a transparent window is usually used as the representative metrics in the studies of combustion oscillation [Micka and Driscoll 2009, Wang et al. 2013]. However, there has been a trade-off between the acquisition rate and the storage of a commercial high speed camera. It is difficult to cover the full length of an acceleration experiment of 10 seconds with repetition rate exceeding a few thousand frame-per-second (fps), which significantly affects the understandings of highly transient flame behaviour. In addition, in practical propulsion systems, a transparent window is not an option, which leads to the development of a passive fibre optical flame sensor that is designed to detect broadband flame light emission. The developed flame sensor resolves flame behavior at the scale of microseconds and covers the full length of an acceleration experiment of 10 seconds. Quantitative flame location is defined from the newly developed instrumentation [Lian et al. 2018] and is adopted here to characterize combustion oscillation. This paper is organized as follows: Experimental facility and the newly developed instrumentation are introduced in Section 2. Definition of flame location and its statistical time series analysis are detailed in Section 3, followed by summaries of the new findings and outlook for future work in Section 4.

[1] *Institute of Mechanics, Chinese Academy of Sciences. No.15 Beisihuanxi Road, Beijing, China, 100190. Email: hlian@imech.ac.cn*

2. Experimental Facility

2.1. Direct-connect supersonic combustion test facility

The CAS transient operation wind tunnel consists of a hydrogen-oxygen vitiator, converging-diverging nozzle with motion controlled cam unit and the test section. The cam profile is designed so that the nozzle contour can be modified to accelerate the flow to the designed Mach number and achieve transient operations. The mass flow rate of the hydrogen and oxygen is controlled in the vitiator to ensure the flow stagnation temperature increases with flight Mach number. The stagnation temperature and pressure are up to 1900K and 4.0MPa with flight Mach number from 4.5 to 6.5. The mass flow rate is 2.0kg/s and the effective test run time is 8 seconds for an optical model combustor and 30 seconds for a water-cooled model combustor. The configuration is illustrated in Fig. 1.

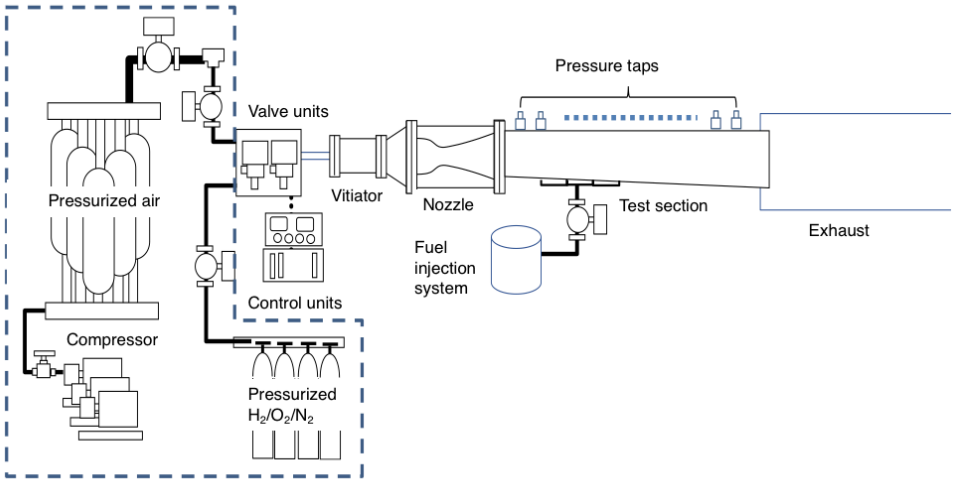

Fig 1. Configuration of the direct-connected supersonic combustion test facility

Experiments have been conducted in a dual-mode model combustor mounted at the test section. The cross section of the constant area isolator measures 80mm×40mm. The model combustor is configured with wall fuel injection and ramped cavity flame holder. The cavity has a depth of 17mm and a length of 65mm. The aft face is angled 22.5°. Kerosene is injected through a row of 6 ports, each of a diameter of 0.3mm. Quartz windows are mounted on each side of the cavity. The ignition source is pilot hydrogen and spark discharge.

2.2. Instrumentations

A spark plug sensor has been developed at CAS, which integrates eight channels of collimating optics and optical fibers to capture engine transients with local flame chemiluminescence emission. The design of such a spark plug sensor has been widely applied in the research of internal combustion (IC) engines [Lian et al. 2017], this is to our knowledge the first time it is developed and adopted in scramjet research. The interpretations of the emission signals are completely different as combustion process in IC engines represents cyclic nature while rapid and continuous combustion occurs in scramjet applications. The cross section of the spark plug is illustratively shown in Fig. 2. The fiber optics are protected from high temperature by sapphire windows, which also ensure probe sealing to prevent deposit build up and loss in light transmissions. The extending fibre attenuation is optimized for broadband transmission of ultra violet (UV) and visible light between 200nm to 600nm, which reduces the effect of black-body radiation close to the near infrared (IR) region. The intensity of broadband emission as well as emission of CH* species occurs in heat release zone are found to monotonically increase with flame temperature [Guethe et al.] with similar ascending slopes. To ensure sufficient sensitivity of the photomultipliers with calibrated gain settings, the intensities of broadband emission I_{bb} are used as indications of flame temperature in this work.

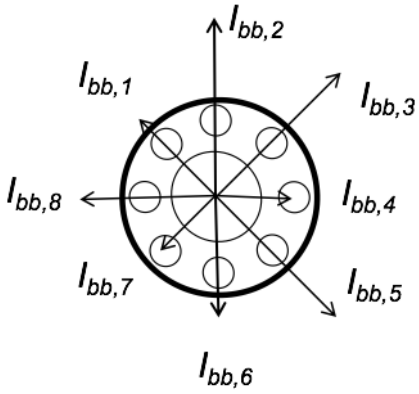

Fig 2. Schematic of the spark plug sensor

In spherical coordinate system, the intensity metric of broadband emission I_{bb} detected by each of the probe is recorded and converted to vector following

$$\mathbf{I_{bb,i}}(\rho_i, \theta_i) = I_{bb,i} \cdot \hat{\boldsymbol{\rho}} + A_{\theta,i} \cdot \hat{\boldsymbol{\theta}}, \ (i = 1,2,\ldots 8). \tag{1}$$

The detected flame location $\boldsymbol{Y}_n$ (n = 1,…,N) is derived from the spatial average of the eight emission vectors as

$$\boldsymbol{Y}_n(\rho_n, \theta_n) = \sum_{i=1}^{8} \mathbf{I_{bb,i}}(\rho_i, \theta_i). \tag{2}$$

The physical meaning of the defined flame location at each discrete time step n is the mass center of the flame temperature represented by the detected intensity of the broadband emission. In this way, the eight-channel flame sensor provides some spatial information while maintaining its high temporal resolution. An example of the defined flame center covering 0.2s from ignition is shown in Fig. 3 with the spark plug sensor installed at the bottom of a cavity flameholder. The color represents experiments with 4 different equivalence ratios and will be discussed in the next Section. The acquisition rate is 200kHz, which yields 40k data points for each colored dataset respectively.

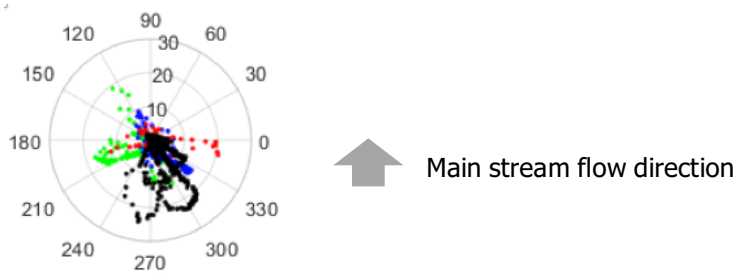

Fig 3. Example of 40k flame locations for 0.2s from ignition.

3. Results and Discussions

The range of flow condition and fuelling options for 4 experimental conditions are summarized in Table 1.

P_o [MPa]	1.4-2.0
T_0 [K]	1200-1800
Ma [-]	2.50-3.08
Fuel Type	RP-3 Kerosene
Fuel Injection	Pilot hydrogen and rear wall fuel injection
Equivalence ratio Φ [-]	Experiment 1: Φ_1= 0.2, Φ_2 = 0.6->0.3 Experiment 2: Φ_1= 0.2, Φ_2 = 0.6 Experiment 3: Φ_1= 0.2, Φ_2 = 0.3 Experiment 4: Φ_1= 0.2, Φ_2 = 0

Table 1. Experimental conditions

For each run, the air was heated by burning hydrogen and oxygen in the vitiator. Four seconds after the vitiator ignition, the main fuel supply was turned on. The pilot hydrogen and the spark discharge were switched on simultaneously and lasted for 1.5 seconds. The equivalence ratio was adjusted according to the main stream mass flow rate during acceleration experiments with varying stagnation pressure, temperature and the Mach number. For the four experiment, the flame locations were measured at 200kHz based on the techniques and interpretation methods described in the previous Section and shown in Fig. 4. The flame location of the four experiments are superimposed with symbols of different colors.

For the first 0.2 second, the flame location is sparsely scattered for all the cases, suggesting the process of flame kernel formation. The ignition process is not of the focus of this work and was discussed in Lian et al. 2018. For the condition of Φ_1= 0.2, Φ_2 = 0, shown in black solid dots, flame development is observed resulting from rapid heat release for approximately 4 seconds and is found to distinguish by the end of the fifth second when the main stream flow accelerates. The distinction is due to insufficient flame holding capability. In comparison, increasing the heat addition in the case of Φ_1= 0.2, Φ_2 = 0.3 would thermally chock the flow that is favourable for flame stabilisation. The fact that the red solid dots are grouped towards the downstream side suggests the flame stabilisation at the downstream cavity. From 6-8 seconds, despite of flow acceleration, the flame moves upstream, which could be caused by the detachment of boundary layers. To fully elucidate the observed flame dynamics requires simultaneous measurements of flow condition and careful examination of its correlation with flame behaviour. The case of Φ_1= 0.2, Φ_2 = 0.6 shown as blue dots is designed to introduce excessive heat addition and the green solid dots represent a dynamic fuelling option with Φ_1= 0.2, Φ_2 = 0.6->0.3. Comparisons on engine thrust measurements would shed light on the optimised fuelling strategy that is favourable for vehicle L/D ratio, however, this is not of the focus of this work.

To further examine and characterise the combustion oscillation behaviour with the goal of identifying appropriate combustion control potentials, the modified Shannon entropy (Wagner et al 2006) is evaluated, which is a quantitative measurement of the randomness of a given time series sequence. It shows the temporal correlation in time series data when discretised into symbols with a specific sequence division *N* and length *L* and is defined as:

$$H_s = -\frac{1}{logn_{seq}} \sum_k p_k log p_k, \tag{3}$$

where, p_k is the probability of observing a sequence *k*, and n_{seq} is the number of different sequences observed in the time series. The entropy equaling 1 (*Hs* = 1) represents a random process while *Hs* < 1 shows the presence of deterministic patterns. In practice, the modified Shannon entropy can be used to: (a) quantify the randomness in time series data and (b) optimize symbol sequence parameters *N* and *L*, with the best representation of temporal correlation occurring in the transient combustion process. The symbol sequence histogram describes the probability of the occurrence of a specific sequence and hence could point to a deterministic mechanism causing this sequence and be used for combustion control purposes. The modified Shannon entropy of ρ_n defined in Eq. (2) for the case of Φ_1= 0.2, Φ_2 = 0.3 is shown in Fig. 5.

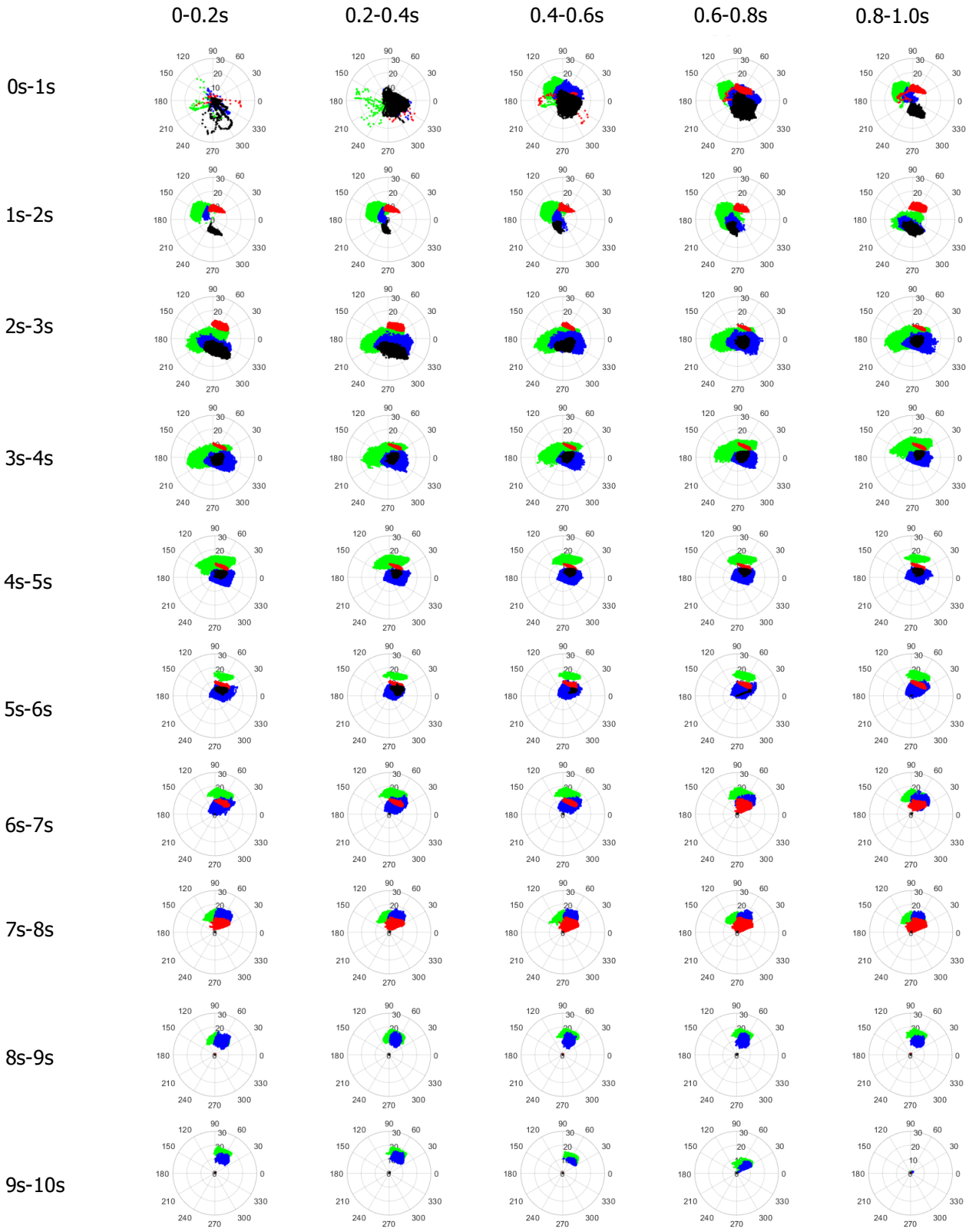

Fig 4. Transient flame behaviour during acceleration experiment. Green: Φ_1= 0.2, Φ_2 = 0.6-0.3; Blue: Φ_1= 0.2, Φ_2 = 0.6; Red: Φ_1= 0.2, Φ_2 = 0.3; Black: Φ_1= 0.2, Φ_2 = 0

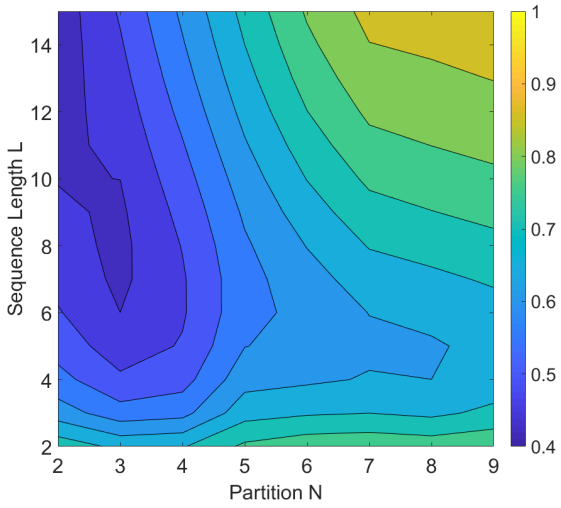

Fig 5. Modified Shannon Entropy for the case of Φ_1= 0.2, Φ_2 = 0.3

First, the minimum modified Shannon Entropy is as low as 0.4 as shown in Fig.5, suggesting a strong existence of deterministic mechanism in the measured transient flame behaviour. This is considered a positive support for further evaluation and development of predictive model of flame dynamics. In addition, the minimum values of the modified Shannon entropy mainly exist with partition of 2 indicates the agreement with the findings of Micka and Driscoll 2009 that there are two stabilisation modes, namely, the cavity stabilisation and the jet wake stabilisation. The corresponding sequence length exceeds 10 suggests the timescale for each mode of stabilisation between 10^1 to 10^2 μs. The transition of the stabilisation modes between ramjet and scramjet operation requires further quantifications.

4. Conclusion

A novel passive optical spark plug probe is developed and applied in a dual-mode scramjet engine during acceleration experiments. The flame dynamics are quantified with the defined flame location. The combustion oscillations evaluated by the modified Shannon Entropy suggests agreement with the widely acknowledged bimodal cavity and jet-wake stabilisation modes. In addition, strong deterministic nature is observed for the first time that positively supports further evaluation and development of predictive models of flame dynamics.

Acknowledgements

The authors appreciate the precious technical support from Mr. Zhanbiao Gao. Financial supports from CAS Facility Development Fund and CAS Hundred Talents Program are acknowledged.

References

1. Curran, E.T., Heiser,W.H., Pratt D. P. Fluid phenomena in scramjet combustion systems. Annu. Rev. Fluid Mech., 28:323–360, 1996.
2. Guethe, F., Guyot,D., Singla,G., Noiray, N., Schuermans, B. Chemiluminescence as diagnostic tool in the development of gas turbines. Appl Phys B, 107:619-636, 2012
3. Lian, H., Martz, J.B., Stefanopoulou, A.G., Zaseck, K., Wilkie, J., Nitulescu, O., Ehara, M., Maldonado, B.P. Prediction of flame burning velocity at early flame development time with high Exhaust Gas Recirculation (EGR) and Spark Advance. J.Eng. Gas Turb. Power, 139:082801, 2017.
4. Lian, H., Martz, J.B., Prakash,N., Stefanopoulou, A.G. Fast computation of combustion phasing and its influence on classifying random or deterministic patterns, J.Eng. Gas Turb. Power, 138:11, 2016.
5. Lian, H., Gu, H.B., Yue, L.J., Chang,X.Y. Investigation of transient ignition characteristics in a model scramjet combustor using spark plug sensor during acceleration experiments. Proceedings of the

19th International Symposium on the Application of Laser and Imaging Techniques to Fluid Mechanics. 2018

6. Micka, D.J., Driscoll, J.F. Combustion characteristics of a dual-mode scramjet combustor with cavity flameholder. Proceedings of the Combustion Institute, 32:2397-2404, 2009
7. Sun, M.B., Wang, Z.G., Geng, H. Flame characteristics in supersonic combustor with hydrogen injection upstream of cavity flameholder. J. Prop. Power, 24(4):688–696, 2008.
8. Wagner, R., Edwards, K., Daw, C., Green, J., Bunting, B., On the nature of cyclic dispersion in spark assisted hcci combustion. SAE Technical Paper, 2006-01-0418, 2006
9. Wang, H.B., Wang, Z.G., Sun, M.B., Qin, N. Combustion characteristics in a supersonic combustor with hydrogen injection upstream of cavity flameholder. Proceedings of the Combustion Institute. 34:2073-2082, 2013